DOI 10.18454/PMI.2016.5.717

UDC 622.619

PNB TYPE LOADER SHOVELING ARM MOTION IRREGULARITY IN DEPENDENCE OF ITS MASS

I.P.TIMOFEEV, A.Yu.KUZKIN
Saint-Petersburg Mining University, Russia

Requirements are formulated on motion trajectory of the front edge of the arm of PNB type loader needed to provide the maximum shoveling of bulk mass under the condition of fitting that trajectory into the dimensions of reception plate. Kinematic schemes are analyzed of mechanisms of shoveling arms. Rational parameters are suggested for that mechanism, which provide a 1.5 times increase of single-time shoveling of bulk load resulting in a 30 % increase of theoretical capacity of the machine.

A technique is presented of defining the area embraced by the complex motion trajectory of the front edge of the arm. A mathematical model is designed of motion of the shoveling arm with curvilinear tail part using the techniques of vector algebra, second order central differences and triangulation. Geometric parameters of the mechanism of work tool of the loader are described by a linear equation yielding the functional dependence of coordinates of the position of front edge of the arm on the turning angle of the leading joint and the parameters of kinematic scheme.

The effect is studied of the total mass of shoveling arm on the irregularity factor of mechanism motion. It is found that redistribution of mass between the work tool and the tail part of the arm within the given total mass of the tool suppresses the motion irregularity factor.

***Key words*:** loader, mechanism, shoveling arm, parameters, capacity, trajectory, factor, mass.

***How to cite this article*:** Timofeev I.P., Kuzkin A.Yu. PNB type loader shoveling arm motion irregularity in dependence of its mass, Zapiski Gornogo instituta. 2016. Vol.221, p.717-723. DOI 10.18454/PMI.2016.5.717

Introduction. Increasing the efficiency of underground mining of mineral resources is directly related to developing new high capacity technology, in particular loading and drilling and loaders that accelerate excavation to prepare the front for cleaning operations.

Currently, parallel to considerable growth of the share of combine sinking stimulated by introduction of powerful high capacity sinking combines of selective action, PNB type loaders with their shoveling arms find wide use [10, 11].

In the course of drilling and blasting operations loading of rock mass is mainly executed by continuous action loaders with shoveling arms. They can handle rock mass of any hardness, according to the scale by M.M.Protodyakonov. Beside that, loaders with shoveling arms are successfully used for tunnel building, cleaning operations and warehousing.

Mechanisms of their work tools and design of shoveling arms are continuously upgraded, new technical solutions emerge [1, 6, 7, 13], as testified by the enormous number of patents and author's certificates. However a technique is missing for comparative assessment of the efficiency of this or that work tool of loaders, of their shoveling arms design; no technique has been designed yet to compare and analyze kinematic schemes of mechanisms of shoveling arms that would help select the most rational one.

Study techniques. Modern continuous action mining loaders of PNB type have their shoveling arms using the following kinematic schemes:

- oscillating crank drive (Fig. 1a);
- oscillating crank gear with straight coulisse (Fig. 1b);
- oscillating crank gear with curvilinear coulisse (Fig. 1c).

The following notations are used in the presented kinematic schemes: r is the connecting rod radius; R is the crank length; d_1, d_2 are the coordinates of crank rotation center with respect to the connecting rod rotation center; β is the angle of deviation of the arm working part from the line of connecting rod; O_1 is the crank rotation center; O_3 is the oscillating crank rotation center.

Shoveling arms of the loaders feature different design shape: linear with its work part deviating from the tail part by angle β (Fig. 1a), bi-segmental, with both the work and the tail parts linear (Fig. 1*b*) and the one with linear work and curvilinear tail parts (Fig. 1*c*).

As rational criteria to assess kinematic schemes we took the shape of the trajectory followed by the front edge of the arm (point C) within the outward dimensions of reception plate and the area embraced by that trajectory.

To achieve the maximum capacity of the machine and the least resistance to the arm sinking into the bulk load, the trajectory followed by the front edge of the arm shall meet the following requirements [2, 14, 17]:

DOI 10.18454/PMI.2016.5.717

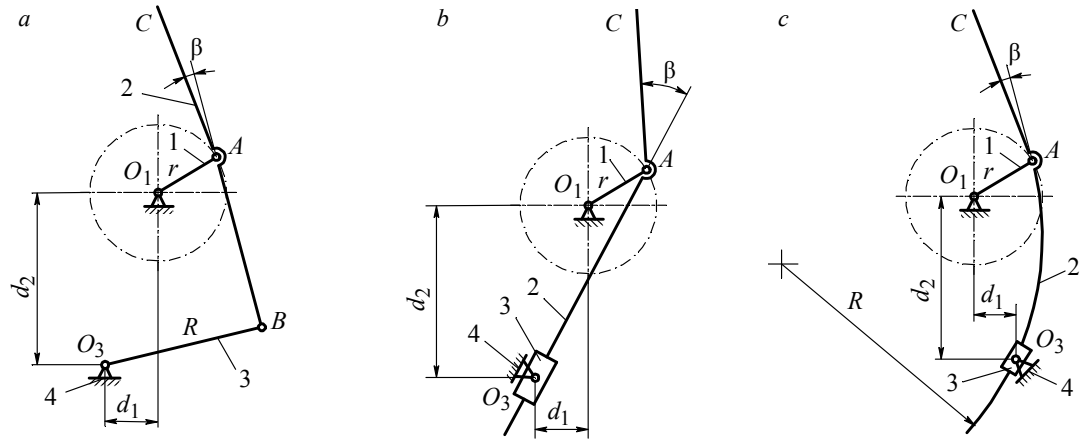


Fig.1. Kinematic schemes for the shoveling arm mechanism

a - oscillating crank drive; *b* – oscillating crank gear with straight coulisse; *c* – oscillating crank gear with curvilinear coulisse; 1 – crank; 2 – (Fig. *a*) connecting rod, (Figs. *b*, *c*) coulisse; 3 – (Fig. *a*) rocker, (Figs. *b* and *c*) slide-bar; 4 – leg

• Fit within the outer dimensions of reception plate of the loader;

• When moving along its penetration leg the arm shall move perpendicular to the front edge of the reception plate and only deviate from that perpendicularity by a minimum angle of ±10° to lower penetration effort;

• The trajectory shall never go outside the side outer dimension of the plate to prevent possible jamming of the arm;

• Along the shoveling leg of the trajectory it shall only reach outside the front edge of the plate by 20-50 mm to loosen the foundation of bulk load by the front edge of the arm in advance of shoveling;

• Along the transportation leg of the trajectory it shall cross the axial line of the reception plate to increase the area embraced by the trajectory and reduce «dead» zones not embraced by the trajectory; also it shall not enter the zone of the conveyor reception window;

• Along the trajectory shall not cross the trajectory of crank butt (point A in Fig.1) along its idle stretch;

• The area embraced by the motion trajectory of the arm front edge shall be as large as possible with the account of the requirements listed above.

To upgrade work tools of loaders of PNB type and produce the newly designed shoveling arms parameters were optimized of their kinematic schemes synthesizing the new mechanisms. A new shape of the shoveling arm (Fig. 1*c*) [13] was proposed along with a rational motion trajectory of the front edge of the arm to improve the machine efficiency. To define motion trajectories of the points of of arm links vector algebra techniques were used [3]. Link rotations were studied using rotation matrices [9], which yield the coordinates of characteristic points. To study the kinematics of mechanisms of shoveling arms analytical and computational techniques were used. Specifically, there exits a matrix called rotation matrix such that multiplying it by the coordinates of a vector one may obtain the coordinates of a new vector rotated by a given angle. A set of turning angles was taken for the computations from 0 to 360° at a step of 1°.

The coordinates of characteristic points of mechanism links were obtained for time moments $t = \varphi/\omega$. Actually the task of digital differentiation was reduced to defining the values of function $y(x)$: $y_1, y_2,..., y_N$ at certain points $x_1, x_2, ..., x_N$.

The coordinates of link points step out as such functions, while $x_1, x_2,..., x_N$ are moments in time.

Then following the second order technique of central differences we calculate the derivative at point $x_к$ is calculated as

$$y'(x_k) = \frac{y_{k-1} - 4y_k + 3y_{k+1}}{x_{k+1} - x_{k-1}}.$$

Differentiating the values of coordinates for point *C* we obtain projections of its linear velocity and acceleration to axes *x* and *y*, and next get their modules and vector directions [5].

To calculate the area of the figure drawn by point *C*, we calculated the area of the polygon that approximates it, retrieved in the course of defining the coordinates of that point. For that purpose the obtained no convex polygon was triangulated using the so-called ear technique.

DOI 10.18454/PMI.2016.5.717

There is a mathematical statement [4] claiming that any polygon has at least two «ears». If one takes an N-polygon and cuts that «ear» off it, an (N-1)-polygon is formed. That procedure may be repeated until the whole polygon will be cut into triangles. When it is cut into triangles, one may calculate the area of each and then sum them up to get an approximation to the area of the figure described by point C.

In case points $A_1(x_1; y_1)$, $A_2(x_2; y_2)$, $A_3(x_3; y_3)$ are apexes of a triangle, then its area is given by the formula:

$$S = \frac{1}{2}\begin{vmatrix} x_1 - x_3 & y_1 - y_3 \\ x_2 - x_3 & y_2 - y_3 \end{vmatrix}.$$

The SW application implemented in the course of computations made i t possible to define parameters of the mechanisms setting 'pure' functions [16] that relate turning angle of the leading link O_1A with the coordinates of characteristic points of the mechanism links. All the necessary computations are done automatically for any modification of the mechanism.

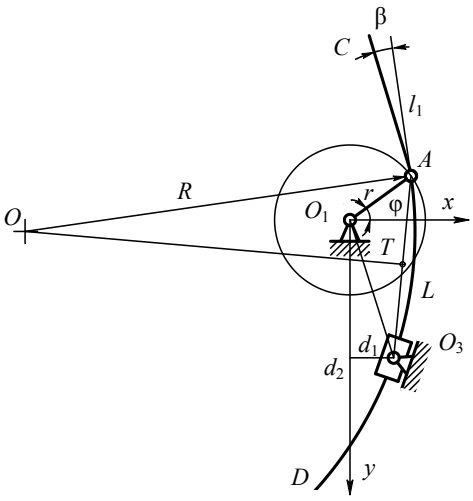


Fig.2. Scheme of the shoveling arm for the mathematical model of oscillating crank gear with a curvilinear coulisse

Fig.2 presents the scheme of such a mechanism, its notations corresponding to those accepted for the mathematical model: r is the length of crank, O_1A; R is the curvature radius of the tail part of the arm, AD; l_1 is the length of the work part of the arm, AC; β is the sharp angle between the extension of the tangent to arc AD at point A and AC; L is the length of arc AD.

The Descartes system of coordinates was chosen so that point O_1 in it would coincide with its origin: the crank rotation axis, while point O_3 would have the coordinates $O_3 = [d_1; d_2]$.

Further study of the mechanism motion follows the assumption that the crank rotates evenly O_1A at a constant angular rate ω, s^{-1}.

The angle of rotation O_1A at the moment t is equal to: $\varphi = \omega t$. The coordinates of point O_1 are $[d_1; d_2]$.

Since the length of vector $\boldsymbol{O_1A}$ is equal to r, its coordinates, hence the coordinates of point A are given by the expression

$$[\boldsymbol{O_1A}] = [A] = \begin{bmatrix} r\cos\omega t \\ r\sin\omega t \end{bmatrix}.$$

Since point O_3 has its coordinates $[d_1; d_2]$, the coordinates of vector $\boldsymbol{O_3A}$ are found from:

$$[\boldsymbol{O_3A}] = [\boldsymbol{O_3O_1}] + [\boldsymbol{O_1A}] = [\boldsymbol{O_1A}] - [\boldsymbol{O_1O_3}] = [A] - [O_3] = \begin{bmatrix} r\cos\omega t - d_1 \\ r\sin\omega t - d_2 \end{bmatrix}.$$

From that one may find the unit normal to it:

$$|\boldsymbol{O_3A}| = \sqrt{\boldsymbol{O_3A}\boldsymbol{O_3A}} = \sqrt{r^2 + d_1^2 + d_2^2 - 2r(d_2\sin\omega t + d_1\cos\omega t)}.$$

Point D lies on the circle of radius R, that goes via the points O_3 and A. To find the coordinates of point D we have first to find the center of the circle. We denote it as O. To find that circle recall that point O is equidistant from points O_3 and A: $|\boldsymbol{O_3A}| = |\boldsymbol{AO}|$. It follows from it that point O lies on the median perpendicular to segment O_3A. We denote the middle of that segment as T: Then, following the fact that point O lies on the median perpendicular to segment O_3A, the condition is met: $\boldsymbol{OT} \perp \boldsymbol{O_3A}$.

The ort of vector $\boldsymbol{O_3A}$ has the coordinates:

$$\boldsymbol{e}_{O_3A} = \frac{1}{|\boldsymbol{O_3A}|} = |\boldsymbol{O_3A}| = \frac{1}{\sqrt{r^2 + d_1^2 + d_2^2 - 2r(d_2\sin\omega t + d_1\cos\omega t)}} \times \begin{bmatrix} r\cos\omega t - d_1 \\ r\sin\omega t - d_2 \end{bmatrix}.$$

From that one may find the unit normal to it:

DOI 10.18454/PMI.2016.5.717

$$\boldsymbol{n}_{\mathrm{O_3A}} = \frac{1}{\sqrt{r^2 + d_1^2 + d_2^2 - 2r(d_2 \sin\omega t + d_1 \cos\omega t)}} \times \begin{bmatrix} r\cos\omega t - d_1 \\ -r\sin\omega t - d_2 \end{bmatrix}.$$

Next we find the coordinates of point T: $\boldsymbol{O_3T} = 0{,}5\boldsymbol{O_3A}$, from which it follows

$$[T] = [O_3] + 0{,}5[\boldsymbol{O_3A}] = \begin{bmatrix} d_1 \\ -d_2 \end{bmatrix} + 0{,}5\begin{bmatrix} r\cos\omega t - d_1 \\ r\sin\omega t - d_2 \end{bmatrix} = 0{,}5\begin{bmatrix} r\cos\omega t + d_1 \\ r\sin\omega t + d_2 \end{bmatrix}.$$

Point O is distanced by R from point A. Triangle OAT is rectangular. Its hypotenuse AO is of length R: $\boldsymbol{AO} = R$.

Cathetus AT is equal to half the length of AO_3 (since point T is the middle of segment AO_3):

$$|\boldsymbol{AT}| = \frac{1}{2}|\boldsymbol{AO_3}| = \frac{1}{2}\sqrt{r^2 + d_1^2 + d_2^2 - 2r(d_2 \sin\omega t + d_1 \cos\omega t)}.$$

Then cathetus TO is of length:

$$|\boldsymbol{TO}| = \sqrt{\boldsymbol{AO}^2 - \boldsymbol{AT}^2} = \frac{1}{2}\sqrt{4R^2 - \left[r^2 + d_1^2 + d_2^2 - 2r(d_2 \sin\omega t + d_1 \cos\omega t)\right]}.$$

Since $\boldsymbol{TO}$ is orthogonal to vector $\boldsymbol{AO}_3$, it is collinear to the vector of the normal $\boldsymbol{n}_{O_3A}$. It means that $\boldsymbol{TO}$ is one of the two vectors $\boldsymbol{TO} = \pm\, \boldsymbol{TO}n_{O_3A}$.

The coordinates of point O may be found from the equality:

$$[O] = [T] + [\boldsymbol{TO}] = \frac{1}{2}\begin{bmatrix} r\cos\omega t + d_1 \\ r\sin\omega t - d_2 \end{bmatrix} \pm \frac{\sqrt{4R^2 - \left[r^2 + d_1^2 + d_2^2 - 2r(d_2 \sin\omega t + d_1 \cos\omega t)\right]}}{2\sqrt{r^2 + d_1^2 + d_2^2 - 2r(d_2 \sin\omega t + d_1 \cos\omega t)}} \times \begin{bmatrix} r\sin\omega t - d_2 \\ -r\cos\omega t + d_1 \end{bmatrix}. \quad (1)$$

Sign election here may be done following the initial conditions. In all our calculations the sign appeared positive. In that case the coordinates of point O have the form (1).

Let us find the tangent at point A to a circle of radius R centered at point O. Since the tangent to a circle is orthogonal to the radius at its touching point, the tangent at point A is orthogonal to radius $\boldsymbol{OA}$. Now we calculate vector $\boldsymbol{OA}$ (1).

The length of vector $\boldsymbol{OA}$ being equal to R, its ort may be found from the formula

$$\boldsymbol{e}_{\mathrm{OA}} = \frac{1}{2R}\begin{bmatrix} r\cos\omega t - d_1 \\ r\sin\omega t + d_2 \end{bmatrix} - \frac{\sqrt{4R^2 - \left[r^2 + d_1^2 + d_2^2 + 2r(d_2 \sin\omega t - d_1 \cos\omega t)\right]}}{2R\sqrt{r^2 + d_1^2 + d_2^2 + 2r(d_2 \sin\omega t - d_1 \cos\omega t)}} \times \begin{bmatrix} r\cos\omega t + d_1 \\ -r\sin\omega t + d_2 \end{bmatrix}. \quad (2)$$

The normal to that vector (hence the ort of the tangent to the circle) is found from the formula (2).

The ort of vector $\boldsymbol{AC}$ is turned by the angle β with respect to the tangent found, therefore its coordinates are $[\boldsymbol{e}_{AC}] = L(\beta)[\tau]$ (2).

Since the vector $\boldsymbol{AC}$ itself is of length l_1, its coordinates have the form (2).

Therefore, the coordinates of point C may be found from the formula

$$[C] = [A] + [\boldsymbol{AC}] = \begin{bmatrix} r\cos\omega t \\ r\sin\omega t \end{bmatrix} + \frac{l_1}{2R}\begin{bmatrix} \cos\beta & -\sin\beta \\ \sin\beta & \cos\beta \end{bmatrix} \times$$

$$\times \left(\begin{bmatrix} r\sin\omega t + d_2 \\ -r\cos\omega t + d_1 \end{bmatrix} - \frac{\sqrt{4R^2 - \left[r^2 + d_1^2 + d_2^2 + 2r(d_2 \sin\omega t - d_1 \cos\omega t)\right]}}{2R\sqrt{r^2 + d_1^2 + d_2^2 + 2r(d_2 \sin\omega t - d_1 \cos\omega t)}} \times \begin{bmatrix} r\cos\omega t - d_1 \\ r\sin\omega t + d_2 \end{bmatrix} \right). \quad (3)$$

Velocity and acceleration of point C are found differentiating the last expression over time.

The analysis of study results. Generalized analysis of mutual effect of the basic parameters of the considered kinematic scheme of working tools of loaders of PNB type [6, 12, 15] on the area inside the

DOI 10.18454/PMI.2016.5.717

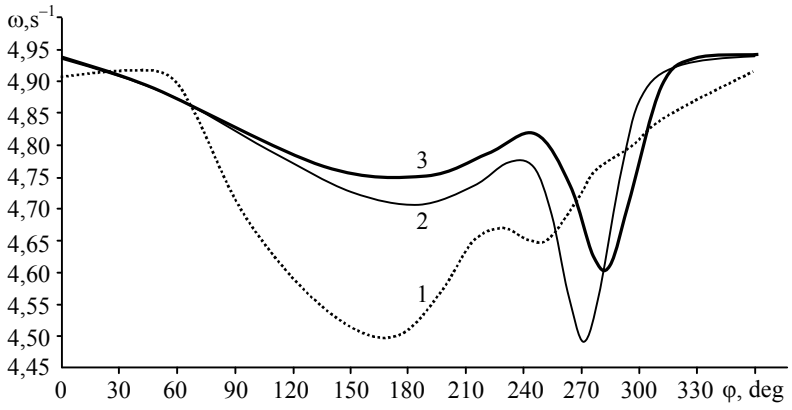


Fig.3. Dependences of $\omega = f(\varphi)$
1 – upgraded oscillating crank drive mechanism; 2 – oscillating crank gear with straight coulisse; 3 – oscillating crank gear with curvilinear coulisse

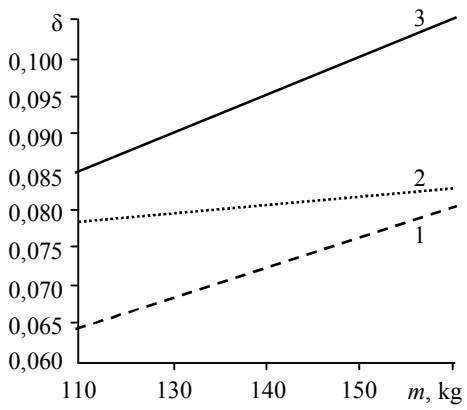


Fig.4. The dependences $\omega = f(m)$
1 – upgraded oscillating crank drive mechanism; 2 – oscillating crank gear with straight coulisse; 3 – oscillating crank gear with curvilinear coulisse

trajectory described by the front edge of the arm and its position on reception plate enabled adopting a rational combination of the mechanism parameters which increases the area inside the trajectory by 1,5 times, thus increasing theoretical capacity of the machine by 30 % (Table 1):

Type of mechanism	r, mm	d_1, mm	d_2, mm	β, deg	R, mm	Area, m^2
Upgraded oscillating crank drive mechanism	250	–180	430	5	–	0.504
Oscillating crank gear with straight coulisse	250	–15	380	30	–	0.470
Oscillating crank gear with curvilinear coulisse	250	90	400	5	1100	0.461

Increase of a single-time shoveled volume of bulk substance results in higher technological load (work resistance) on the work tool of the loader. The technological load formed during various phases of arm motion along its trajectory in the course of interaction with bulk substance is not constant [8].

Assessment of the dynamics of the leading link for the studied schemes was obtained calculating the irregularity factor and its variations.

Fig. 3 presents the graphs of the dependence of angular rate of such a leading link (the crank) ω on the turning angle of the crank φ obtained from the results of computer simulation on the condition the total mass of arm, m = 130 kg, remains constant and corresponds to the respective mass of arm of loaders from the same parametric series, while the ratio of masses of work and tail parts of the arm is 1.0.

The minimum and maximum values of angular rates were: 4.50 and 4.91 s^{-1} for the upgraded oscillating crank drive mechanism; 4.48 and 4.93 s^{-1} for oscillating crank gear with straight coulisse; 4.61 and 4.94 s^{-1} for oscillating crank gear with curvilinear coulisse.

Calculated values of motion irregularity factor for the leading link: δ = 0.085 for the upgraded oscillating crank drive mechanism; δ = 0.0904 for oscillating crank gear with straight coulisse and δ = 0,0675 for oscillating crank gear with curvilinear coulisse. The irregularity factor was calculated as

$$\delta = \frac{\omega_{max} - \omega_{min}}{\omega_{cp}},$$

where ω_{max} and ω_{min} are the maximum and minimum angular rate over a cycle of mechanism motion, s^{-1}; ω_{cp} is the average angular rate over the mechanism motion cycle, s^{-1}.

Note that for the oscillating crank gear with curvilinear coulisse the motion irregularity factor is 1.4 times less than the one for the oscillating crank gear with linear coulisse and 1.3 times less than the one for the upgraded oscillating crank drive.

The arm mass, m was taken within the range of 120-160 kg for loaders of different type and size.

The results of studying the effect of total mass of machine arm, m on the motion irregularity factor for the mechanisms δ of the considered kinematic schemes are presented in Fig.4.

DOI 10.18454/PMI.2016.5.717

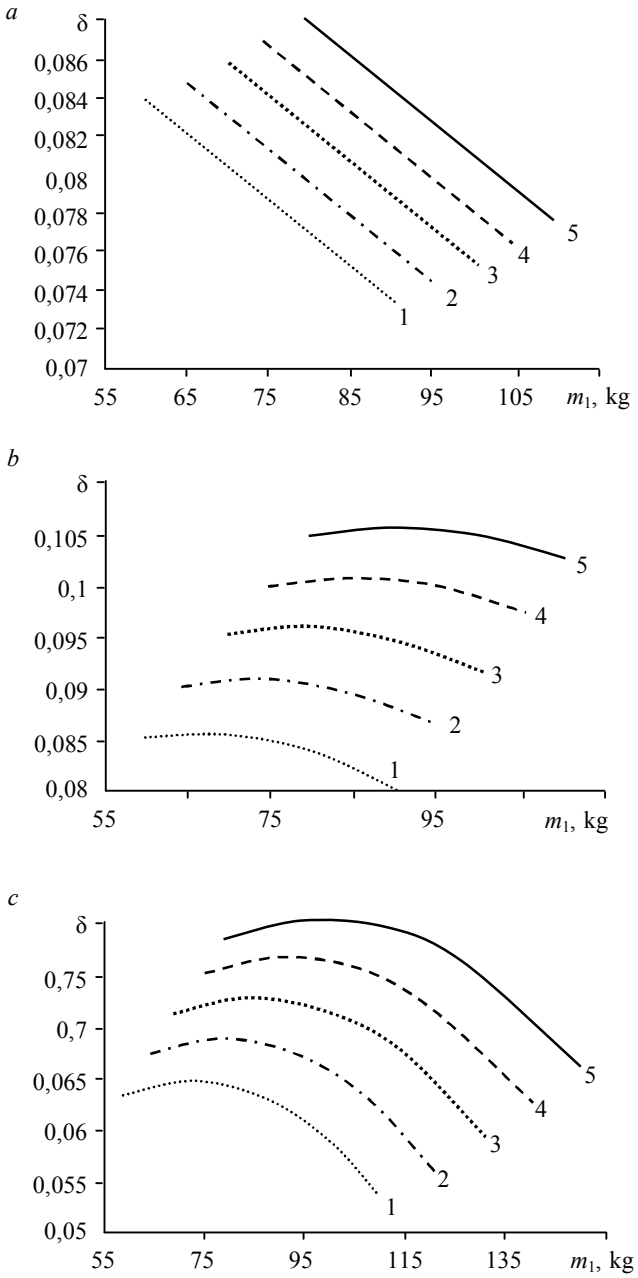


Fig.5. Dependences $\delta = f(m_1)$ for the oscillating crank drive mechanism (*a*); oscillating crank gear with straight coulisse (*b*); oscillating crank gear with curvilinear coulisse (*c*)
1– m =120 kg; 2 – 130; 3 – 140; 4 – 150; 5 – 160

A linear dependence $\delta = f(m)$ was found for every studied scheme. Note that the scheme of oscillating crank drive demonstrates quite a weak change in motion irregularity δ with the arm mass, m increasing, so that it is 0.0726 for a 120 kg arm and 0.0826 for a 160 kg one; for the oscillating crank gear with straight coulisse it is 0.0851 for a 120 kg arm and 0.1054 for a 160 kg one; for the oscillating crank gear with curvilinear coulisse it is 0.0645 for a 120 kg arm and 0,0804 for a 160 kg one.

The motion irregularity factor was found to decrease δ with the shift of the center of masses of shoveling arm towards its tail part. With the mass of tail part of the arm, m_1 increasing the motion irregularity factor of the mechanism lowers for every assumed mass m.

Fig.5 *a* presents the dependences of the motion irregularity factor δ in dependence of the mass of tail part of the arm, m_1 for the oscillating crank drive mechanism.

Study results have demonstrated that increasing the mass of tail part of the arm, m_1 with respect to the mass of work part, m_0 by a factor of 1.5 lowers the motion irregularity factor by 15 % for every value of arm mass.

Fig.5 *b*, *c* present the dependences of motion irregularity factor δ of the mass of tail part of the arm, m_1 for the oscillating crank gear with straight coulisse and the oscillating crank gear with curvilinear coulisse, respectively. A parabolic dependence was found of changes in the motion irregularity factor δ on the mass of tail part of the arm, m_1 for every studied mechanism. Increasing the mass of tail part of the arm, m_1 lowers the crank motion irregularity factor.

The analysis of the graphs presented has shown that with the increase of mass of tail part of the arm, m_1 the motion irregularity factor for the mechanism δ lowers for every adopted value of arm mass, m and every studied mechanism.

Conclusions

1. The analysis of kinematic scheme of work tool mechanism of PNB type loader has demonstrated that the parameters of oscillating crank drive mechanism of the shoveling arm fail to provide a trajectory that would meet in full the target functions and the limitations set.

2. Mathematical model of work tool of the loader operating by shoveling arms is described by a linear equation that defines the functional dependence of coordinates of the position of front edge of the arm on the turning angle of its leading link and geometric parameters of its kinematic scheme.

3. Motion irregularity factors of the mechanism for the arm mass corresponding to the mass of basic model of PNB type loader (m = 130 kg) are: 0.085 for the oscillating crank drive scheme; 0.0904 for the oscillating crank gear with linear coulisse; 0.0675 for the oscillating crank gear with curvilinear coulisse.

4. A linear dependence is found of motion irregularity factor δ on the arm mass. Increasing of the arm mass, m from 120 to160 kg results in a change of the motion irregularity factor from 0.0726 to 0.0826 for the

DOI *10.18454/PMI.2016.5.717*

oscillating crank drive mechanism; from 0.0851 to 0.1054 for the oscillating crank gear with linear coulisse and from 0.0645 to 0.0804 for the oscillating crank gear with curvilinear coulisse.

5. A parabolic dependence of motion irregularity factor is found for the studied mechanisms on the mass of tail part of the arm. Increasing the mass of tail part of the arm, m_1 lowers the motion irregularity factor.

6. The motion irregularity factor is found to be 1.4 times lower for oscillating crank gear with curvilinear coulisse than the one for oscillating crank gear with linear coulisse and 1.3 times lower than the one for oscillating crank drive.

REFERENCES

1. *Afonina N.B.* On developing a technique to study loading tools of headers with shoveling stars. Gornoe oborudovanie i jelektromehanika. 2013. N 2, p.25-30 [in Russian].

2. *Vasil'eva M.A.* Increasing the capacity of loader via upgrades to its shoveling arm mechanism: Avtoref. dis…kand. tehn. nauk. Nacional'nyj mineral'no-syr'evoj universitet «Gornyj». St. Petersburg, 2012, p.21 [in Russian].

3. *Verzhbickij V.M.* Foundations of Numerical Techniques: Moscow: Vysshaja shkola, 2002, p.840 [in Russian].

4. *Volkov E.A.* Numerical techniques. Moscow: Nauka, 1987, p.248 [in Russian].

5. *Evgrafov A.N.* Computer aided computing and designing machine mechanisms. SPbGTU. St. Petersburg, 1992, p.80 [in Russian].

6. *Otrokov A.V.*, *Hazanovich G.Sh.*, *Kolesnichenko I.E.*, *Hazanovich V.G.* On the issue of systematizing design and kinematic schemes of continuous operation loading tools. Sovremennye problemy nauki i obrazovanija. 2014. N 4. URL: www.science-education.ru/118-13857 [in Russian].

7. *Kravchenko P.D.*, *Rjumin I.F.* Effect of irregularity of motion of the shoveling arm on loading capacity and power consumption. Trudy Novocherkasskogo politehnicheskogo in-ta. 1970. Vol.218, p.119-125 [in Russian].

8. *Krisachenko E.A.* Studying the process of interaction of work tools of loaders featuring paired shoveling arms with piled lumpy bulk substance: Avtoref…kand. tehn. nauk. JuRGPU. Novocherkassk. 1971, p.21 [in Russian].

9. *Lojcjanskij L.G.*, *Lur'e A.I.* A Course of Theoretical Mechanics. V 2-h tomah. Vol.2. Moscow: Nauka, 1983, p.640 [in Russian].

10. *Malevich N.A.* Mining heading machines and complexes. Moscow: Nedra, 1980, p.384 [in Russian].

11. Machines and equipment for horizontal and tilt mining excavation. Pod obshhej red. B.F.Bratchenko. Moscow: Nedra, 1975, p.416 [in Russian].

12. *Belous N.A.*, *Kuz'kin A.Ju.*, *Sokolova G.V.*, *Timofeev I.P.* Substantiating rational parameters of mechanisms for shoveling arms of underground mine loader. Sovremennye problemy nauki i obrazovanija. 2014. N 4. URL: www.science-education.ru/118-13901 [in Russian].

13. *Timofeev I.P.*, *Sokolova G.V.*, *Belous N.A.*, *Kuz'kin A.Ju.*, *Kolton G.A.* Patent N 2560013 RF. Loader. Opubl.20.08.15. Bul. N 23 [in Russian].

14. *Timofeev I.P.*, *Vasil'eva M.A.*, *Kuz'kin A.Ju.* Effect of geometric parameters of the mechanism of shoveling arms of mine loaders on their capacity. Materialy Mezhdunarodnoj nauchno-prakticheskoj konferencii molodyh uchenyh i studentov «Opyt proshlogo – vzgljad v budushhee»; TulGU. Tula, 2011, p.56-58 [in Russian].

15. *Timofeev I.P.*, *Belous N.A.*, *Kuz'kin A.Ju.* Optimization of kinematic parameters of shoveling arm mechanism for PNB type loaders. Zapiski Gornogo instituta. 2014. Vol.209, p.13-17 [in Russian].

16. *Fild A.*, *Harrison P.* Functional Programming. Moscow: Mir, 199, p.637 [in Russian].

17. *Hazanovich G.Sh.*, *Kargin R.V.*, *Nosenko A.S.* Theoretical studies of load formation in the cline pulling transportation tool of the digger off-loader. Nauchno-tehnicheskie i social'no-jekonomicheskie problemy Rossijskogo Donbassa: Materialy 49-j nauchno- proizvodstvennoj regional'noj konferencii; SKNC VSh. Rostov-na-Donu. 2000, p.109-114 [in Russian].

***Authors*: I.P.Timofeev,** *Dr. of Engineering Sciences*, *Professor*, *partim@mail.ru* (*Saint-Petersburg Mining University*, *Russia*), **A.Yu.Kuzkin,** *PhD in Engineering Sciences*, *Associate Professor*, *kuskinay@bk.ru* (*Saint-Petersburg Mining University*, *Russia*).

The paper was accepted for publication on 28 April, 2016.